

Wear behavior of Al–Cu and Al–Cu/SiC components produced by powder metallurgy

Adel Mahamood Hassan · Ahmad Turki Mayyas ·
Abdalla Alrashdan · Mohammed T. Hayajneh

Received: 4 April 2008 / Accepted: 28 May 2008 / Published online: 29 June 2008
© Springer Science+Business Media, LLC 2008

Abstract In the present study, the dry sliding wear behavior of some powder metallurgy (P/M) Al–Mg–Cu alloys with different weight percentage of Cu (0, 1, 2, 3, 4, and 5 wt%) and corresponding metal matrix composites reinforced with 5 or 10 vol% silicon carbide particles (SiC) have been carried using pin-on-disk apparatus. The tested specimens were tested against hardened steel disk as a counter face at room conditions (~ 20 °C and $\sim 50\%$ relative humidity). The normal load was 40 N and sliding velocity of counter face disk was 150 rpm (0.393 m/s) and total testing time of 60 min, which corresponds to a distance of 1414 m. Generally, both hardness and wear resistance were enhanced by the addition of Cu and/or SiC to the Al-4 wt% Mg alloy. The formations of mechanically mixed layer (MML) as a result of material transfer from counter face disk to the samples and vice versa were observed in all tested specimens.

Introduction

Metal-matrix composites (MMCs) are a new class of material that consists of a nonmetallic phase distributed in a metallic matrix with properties that are superior to use of the constituents. According to many authors like Abouelmagd [1] and Ahlatci et al. [2] the most commonly used methods for manufacturing of MMCs are casting techniques and powder metallurgy (P/M) techniques.

Aluminum matrix composites (AMCs) refer to the class of light weight high performance aluminum centric material systems. The reinforcement in AMCs could be in the form of continuous/discontinuous fibers, whisker, or particulates, in volume fractions ranging from a few percent to 60% or more, for example Candan and Bilgic [3] investigated corrosion behavior of Al-60 vol% SiC_p composites which was produced by pressure infiltration technique. Aluminum-based alloys are usually reinforced with Al₂O₃, SiC, and graphite. The major advantages of AMCs compared to unreinforced materials are as follows: greater strength, improved stiffness, reduced density, good corrosion resistance, improved high-temperature properties, controlled thermal expansion coefficient, thermal/heat management, enhanced and tailored electrical performance, improved wear resistance, and improved damping capabilities.

Increased demand for light weight components, primarily driven by the need to reduce energy consumption in a variety of societal and structural components, has led to increased use of aluminum. Additionally, the cost of fabrication coupled with a need to improve part recovery has carried significant growth in the net-shaped component manufacturing processes. Among the various methods to fabricate metal matrix composites, P/M method is one of the attractive production techniques for production of MMCs. Aluminum P/M offers components with exceptional mechanical and fatigue

A. M. Hassan (✉) · A. T. Mayyas · A. Alrashdan ·
M. T. Hayajneh
Industrial Engineering Department, Faculty of Engineering,
Jordan University of Science and Technology, P.O. Box 3030,
Irbid 22110, Jordan
e-mail: adel@just.edu.jo

A. T. Mayyas
e-mail: mayyas111@just.edu.jo

A. Alrashdan
e-mail: alrash@yahoo.com

M. T. Hayajneh
e-mail: hayajneh@just.edu.jo

properties, low density, corrosion resistance, high thermal and electrical conductivity, excellent machinability, good response to a variety of finishing processes, and which are competitive on a cost per unit volume basis according to Torralba et al. [4]. Eksi and Saritas [5] found that aluminum P/M parts can be further processed to eliminate porosity and improve mechanical properties either by cold or hot working methods to obtain properties comparable to those of conventional cast aluminum products. Many applications of Al P/M in automotive industry include connecting rods, cams, and races for tapered roller bearing, valve seat, and automotive industries.

Reinforcement of aluminum alloys with Al_2O_3 or SiC has generally been observed to improve wear and abrasion resistance as described by many former researchers. Sawla and Das [6] studied the abrasive wear behavior of various Al alloys, such as Al–Mg, Al–Cu, and Al–Zn–Mg, which were reinforced with hard particles; they found that the wear rates of these hard particle composites are significantly lower than the wear rates of corresponding base alloys. Das et al. [7] found that wear resistance properties of Al–4.5 wt% Cu alloy improved significantly after addition of alumina and zircon particles. However, there is an increasing demand to develop new materials, for brake lining and clutch facing to withstand the technological progress in industry, instead of the conventional one based on asbestos [8]. Friction materials used as brake linings and clutch facing are commonly made from asbestos or other inorganic fibers and ingredients which include metallic powders and mineral filler as well as the binder in the form of a resin [8]. Frictional materials containing conventional organic binding agents exhibit poor frictional stability. P/M of Al MMCs is produced to overcome the poor thermal resistance and withstand higher thermal stresses as well as increasing wear resistance [1, 8].

The addition of small quantities of magnesium to Al/SiC composite system is recommended in order to improve the wettability and bonding strength between metal matrix and reinforcement particles, as well as to reduce the porosity volume fraction in the produced components [2, 9]. The addition of wetting agent is used in the casting methods, but in this study we introduce 4 wt% Mg in the P/M Al–Cu/SiC composite components to enhance bonding strength.

The present study aims to investigate the abrasive wear behavior of some Al–4 wt% Mg–Cu alloys and Al–4 wt% Mg–Cu/SiC composites using pin-on-disk apparatus under ambient conditions.

Experimental setup and procedure

Materials

The powders used in fabricating alloys and composite in this study were: pulverized and nitrogen flushed aluminum

powder with an average size of 75 μm and a purity of 99%, magnesium powder with an average size <300 μm and a purity of 99%, copper powder with an average size of 63 μm and a purity of 99.5%. The SiC ceramic particles of size 75 μm were selected for this experiment.

Processing

Aluminum powder is mixed with alloying metal powders (copper and magnesium) and reinforcement powder (silicon carbide) in precisely controlled quantities. Copper was added in six levels with different weight percentages of (0, 1, 2, 3, 4, and 5 wt%) and fixed weight percentage of magnesium (4 wt%). Specific quantities of silicon carbide particles of 5 and 10 vol% were added to the matrix alloys. Then the premixes were compacted using precision metal die with Ø 20 mm in the laboratory vertical unidirectional press with a capacity of about 400–410 kN (\sim 128 MPa) to yield a green compact. Aluminum premixes exhibit excellent compressibility and yield high density parts at low compaction and ejection pressures. Premixes can be compacted to 90% of theoretical density according to [5, 10]. The green compacts were sintered in a controlled atmosphere at closely regulated temperature 530 $^\circ\text{C}$ for 60 min as suggested by Yamagushi et al. [11]. This process metallurgically bonds the powder particles together and develops the desired physical and mechanical properties. Successful sintering of Al-based powders was accomplished in argon-rich environment since the sintering process of aluminum powder is difficult to achieve because the aluminum oxide is not reduced inside the furnace atmosphere at typical sintering temperatures. Finally, the obtained bars were turned to small specimens of 4 mm diameter and 25 mm length to be used in the wear testing machine.

Wear test

Dry wear test was carried out under ambient conditions (20–22 $^\circ\text{C}$ and \sim 50 \pm 5% relative humidity) using pin-on-disk wear testing machine as shown in Fig. 1. Prior to testing, the samples were firstly grounded against number 800 SiC grit papers, washed thoroughly with ethanol, dried, and then weighed accurately using electric balance with 0.1 mg accuracy. The counter face disk was made from medium carbon steel of 50 mm diameter and 10 mm thickness, and hardened to 645 HV and polished to final surface roughness of 0.22 μm .

The specimens were tested at 40 N normal loads (corresponding to a mean contact pressure of 3.18 MPa) and a sliding speed of 150 rpm (0.393 m/s). Friction coefficients were recorded continuously using a calibrated force transducer. The coefficient of friction of the samples was

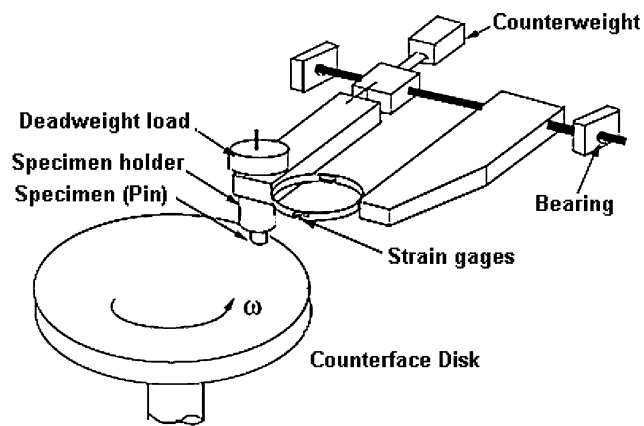


Fig. 1 Schematic of the pin-on-disk apparatus

calculated by dividing the friction force by the normal load. Hardness test was carried out using Vickers microhardness tester with 100 gf and 10-s retention time with at least three indentations of each sample and then the average values were taken to calculate hardness number. The wear test was carried out in increment manner with 10 min interval per increment (corresponding to 236.5 m) and 60 min as a total testing time (corresponding to 1414 m). After each period of the test (i.e., 10 min) the test machine was switched off and the specimen and counter face disk were removed, cleaned with organic solvents to remove traces of oil or other surface contaminants, dried, and then weighed to determine the mass loss. The mass loss of the specimen was used to study the effect of copper and silicon carbide addition on the wear resistance of the composite materials under consideration.

Metallographic samples were prepared using the standard metallographic procedure of grinding, polishing, then etched with standard aluminum etching solutions and examined by optical microscope (Olympus). Scanning electron Microscope (SEM) (Quanta 200) equipped with energy dispersive X-ray spectroscopy (EDS) (EDAX) was used to observe and analyze the worn surfaces.

Results and discussions

Wear mechanism

The typical microstructures of some investigated Al-4 wt% Mg–Cu alloys and Al-4 wt% Mg–Cu–SiC components are shown in Fig. 2 and the associated material properties are given in Appendix.

Throughout the testing period, weight loss of the investigated alloys decreased with increasing Cu content of the matrix (up to 5 wt% in this work) due to the increase of the matrix hardness. Many researchers found that the wear loss is inversely proportional to the hardness of alloys [2, 12,

13]. Their results are comparable to the results we found in this research. The results show that the hardness of Al-4 wt% Mg alloy increased by the addition of Cu content up to 5 wt% as shown in Appendix. The plots of wear loss versus sliding time for the Al-4 wt% Mg–Cu alloys and Al-4 wt% Mg–SiC composites are shown in Figs. 3 and 4. The mass losses in wear test of the copper-containing alloys were less than that for copper-free alloys in general. Moreover, the mass loss decreases with increasing copper content for the percentages considered in this study. The lowest value of mass loss of Al-4 wt% Mg–Cu alloys was attained by the addition of 5 wt% Cu. Also, it was observed that wear rate of Al-4 wt% Mg–Cu alloys decreases after addition of silicon carbide particles. This is attributed to the increase in hardness of the material due to the presence of hard ceramic particles as well as the role of these hard particles, which act as load bearing elements. However, in the case of aluminum-based composites; relatively harder particulate matrix is in contact with the counter face disk rather than soft matrix of Al–Mg–Cu alloys [2].

Moreover, Figs. 3 and 4 show variation of wear rate with sliding distance for the Al-4 wt% Mg–Cu alloys and Al-4 wt% Mg–SiC composites. In the case of Al-4 wt% Mg–Cu alloys it was observed that wear rate increases initially and then gradually decreases with sliding distance (in order of mgs which can be shown from the slope of cumulative mass loss). This refers to the run-in period in the early stage of wear test. At the initial stage of sliding, the alloy matrix is softer compared to the later stage, as the alloy matrix gets strain hardened due to continuous sliding under an applied load after a certain sliding distance [7]. However, such strain hardening effect is significantly observed in the case of Al-4 wt% Mg–Cu alloys compared to the Al-4 wt% Mg–SiC composites. The absence of strain hardening of the matrix during the initial sliding in the case of composites is due to the existence of pre-strained matrix. It is known that the coefficient of thermal expansion (CTE) of ceramic particles is less than that of aluminum alloy [7]. The presence of pre-strained matrix in the MMCs will cause an enormous amount of dislocations at the particle–matrix interface during solidification process, which further increases the matrix hardness [7, 14]. Figure 4 shows that the wear rate of aluminum-based composites is almost constant with sliding distance, which attributed to the uniform wear of surface during the test.

Worn surfaces characterization

The friction between sliding surfaces is due to the combined effects of adhesion between flat surfaces, plowing by wear particles and hard asperities, and asperity deformation, and in due course, wear grooves and scratches are

Fig. 2 Optical micrographs of some alloys and composites used in this study: (a) Al-4 wt% Mg; (b) Al-4 wt% Mg–5 vol% SiC; (c) Al-4 wt% Mg–4 wt% Cu; (d) Al-4 wt% Mg–2 wt%Cu–5 vol%SiC. (200×)

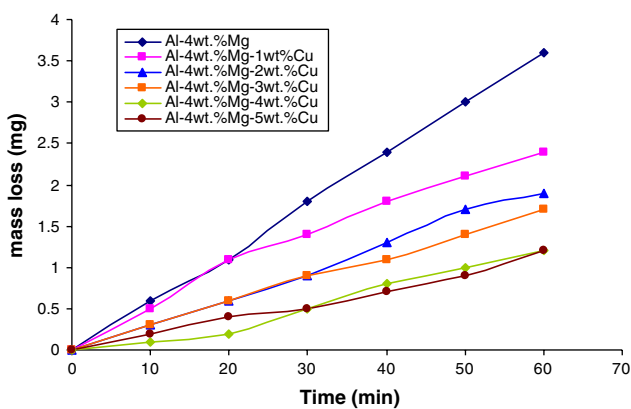
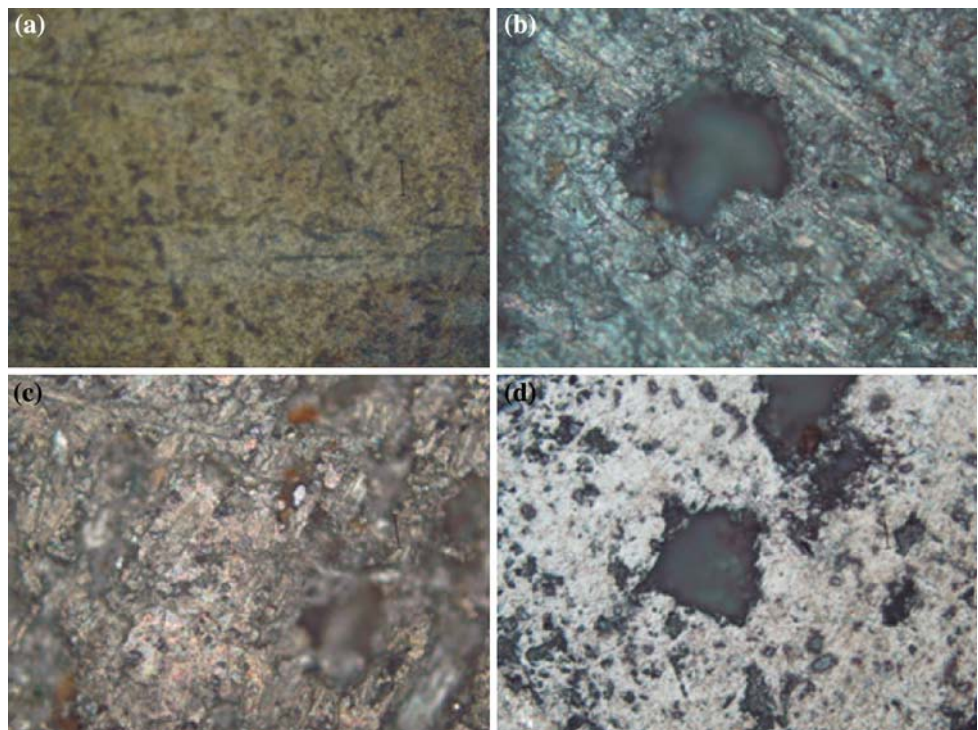


Fig. 3 Cumulative mass loss versus testing time of Al-4 wt% Mg–Cu alloys

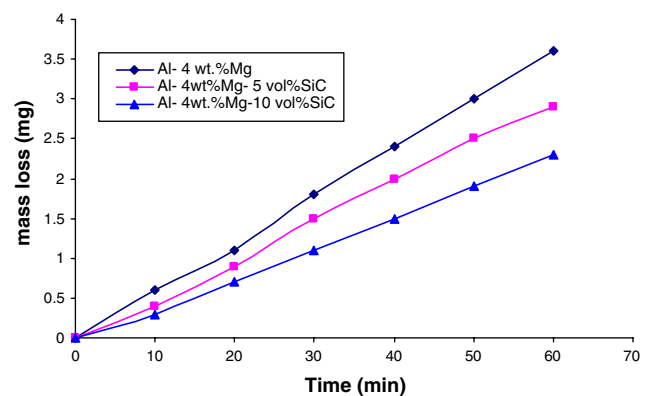


Fig. 4 Cumulative mass loss versus testing time of Al-4 wt% Mg–SiC composites

generated. The major portion of grooves is formed along sliding direction; the depth and width of these grooves and scratches generally control the amount of material removed from the specimen surface. Typically severe grooves are formed in unreinforced alloys compared to those formed in reinforced alloys with SiC particles. The overall wear depends on the ability of the harder asperities of counter face disk to penetrate into the specimen surface and the extent of penetration.

The severity of abrasion in the case of alloy is due to the depth of penetration, which is governed by the hardness of the specimen surface and applied load. But, in the case of composite, the depth of penetration of the harder asperities is primarily governed by the protruded hard ceramic

reinforcement particles. Thus, the major portion of the applied load is carried by SiC particles. This is attributed to the action of the effective load on the individual particle; if the load gets increased above its flexural strength, the particles get fractured. Parts of the removed SiC particles lodge between the two rubbing surfaces, possibly leading to three-body abrasion and abrade one or both of these surfaces. The entrapped SiC particles contribute to the surface roughness and consequently increase the coefficient of friction [14–18]. Figure 5 shows schematic illustration of three-body abrasion model. The tribofilm contains debris from specimen and counter face steel disk. Figure 6 shows the typical coefficient of friction diagram for some components tested in this study.

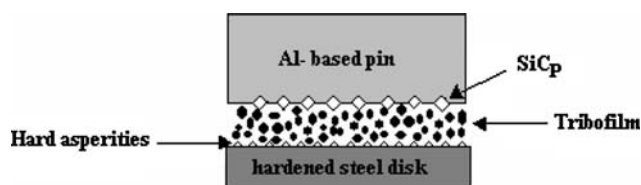


Fig. 5 Illustration of three-body abrasive wear

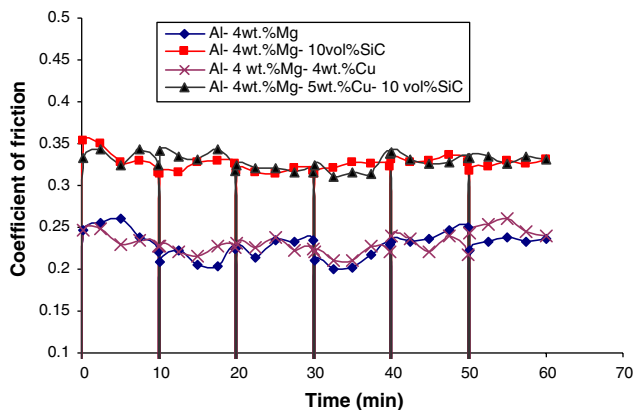


Fig. 6 Coefficient of friction for some alloys and composites used in this experiment

SEM micrographs show the direction of abrasion. Significant cracking action of weak regions was observed in the case of Al-4 wt% Mg–Cu alloys. These cracks indicate the effect of plastic deformation and cold working during the wear, as they appear parallel to the sliding direction. Typical worn surface of Al–Mg–Cu alloys are shown in Figs. 7a and 8a; these worn surfaces are characterized by smearing and scratches along the sliding direction. Deep grooves and ductile fragments may result in microwelding spots, which appear as ductile fragment welded to ductile

material of aluminum matrix alloy. Figure 7a is a secondary electron image (SEI) from the wear tracks showing the surface topography and Fig. 8a is backscattered electron micrograph (BSE) of the worn surfaces showing the abrasion tracks.

In aluminum matrix composites, when the matrix surrounding SiC particles is worn away due to abrasion by harder counter face steel asperities, the ceramic particles loosen away or are entrapped between two contact surfaces. The trapped SiC particles and worn metal debris from AMCs and counter face disk form the tribofilm. This tribofilm contains hard ceramic particles that result in three-body abrasion mechanism and hence increases the coefficient of friction [14–16]. Figures 9a and 10a show the worn surfaces of AMCs containing SiC particles. In the case of Al–Mg–Cu alloys, the tribofilm mainly consists of metal debris and behaves as a lubricating layer, such layer appears as shown in Fig. 10. The worn surface shows groove formation, damaged regions, and cracks propagation along the longitudinal and transverse directions. EDS analysis conducted on the worn surfaces revealed the formation of mechanically mixed layer (MML) due to the transfer layers from the counter face, such as Fe, Ni, Cr, Mo, and Si. It seems to be a MML composed of debris particles, probably fractured and comminuted, coming from both sides of the contact. The presence of Fe and O₂ indicates oxidation effect resulted from higher temperatures at the contact region. These oxides are FeO and Fe₂O₃ and behave as a solid lubricant, thus decreasing the coefficient of friction [16, 18]. Since Fe-rich transfer layer acts as a solid lubricant and prevents direct contact between the samples and counter face during wear testing, thick transfer layer is much more effective in improvement of metal–metal wear resistance. The characterization of worn surface

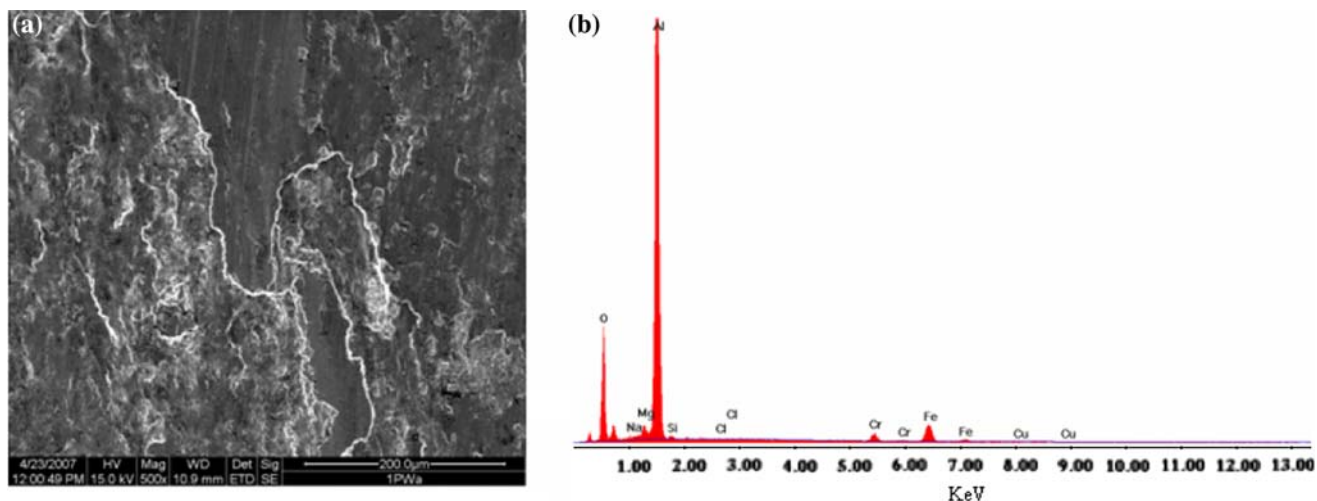


Fig. 7 SEM micrograph of worn surface of Al-4 wt% Mg alloy (a); and its corresponding EDS analysis (b)

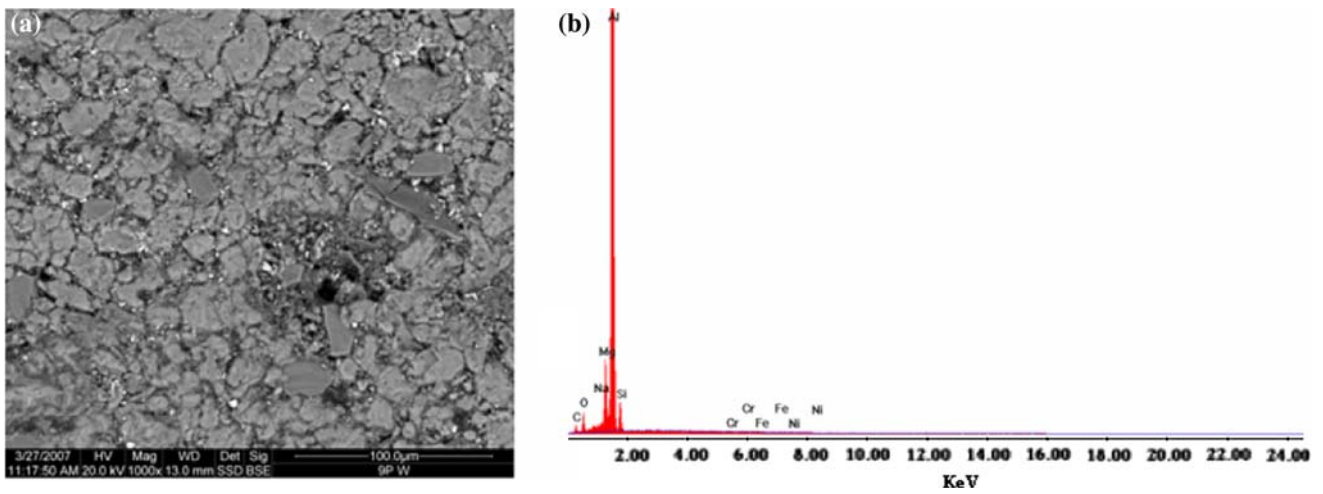


Fig. 8 SEM micrograph of worn surface of Al-4 wt% Mg-4 wt% Cu alloy (a); and its corresponding EDS analysis (b)

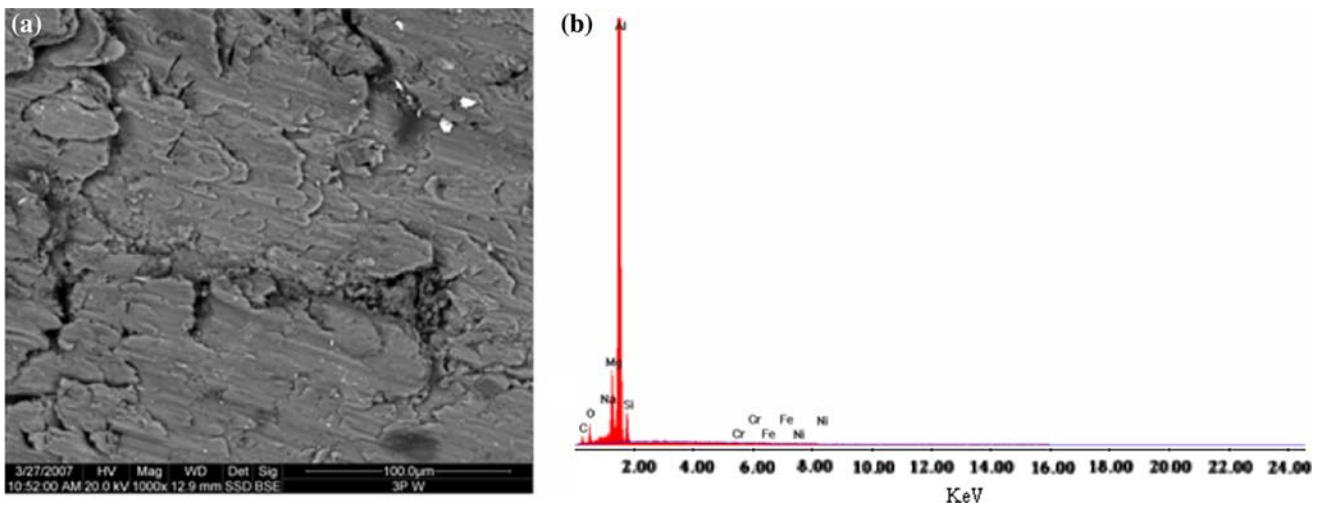


Fig. 9 SEM micrograph of worn surface of Al-4 wt% Mg-10 vol% SiC composite (a); and its corresponding EDS analysis (b)

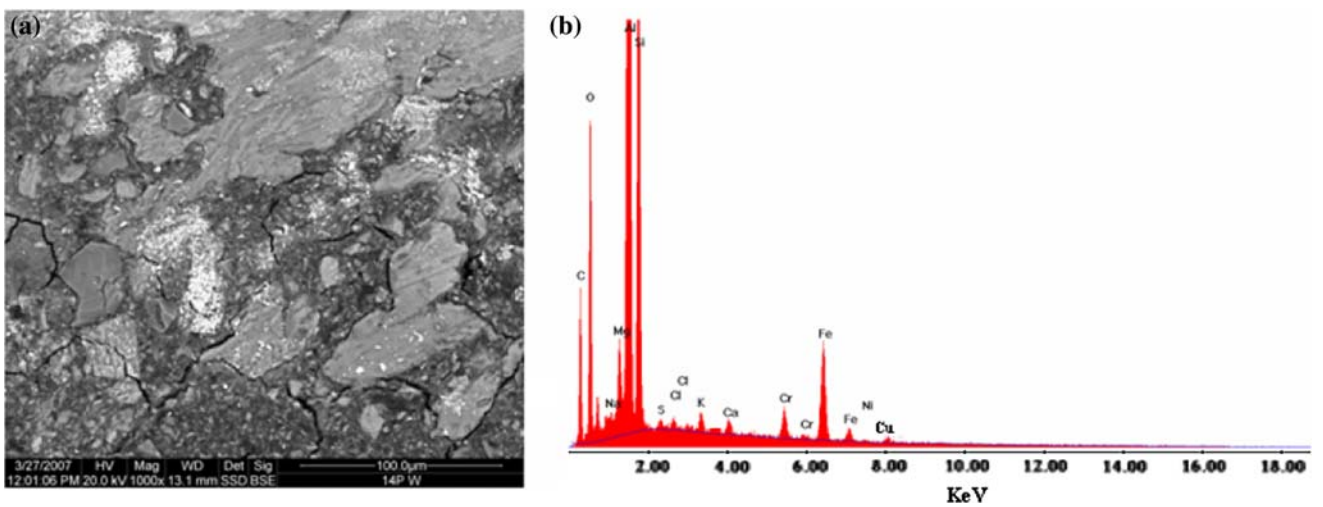


Fig 10 SEM micrograph of worn surface of Al-4 wt% Mg-4 wt% Cu-10 vol% SiC composite (a); and its corresponding EDS analysis (b)

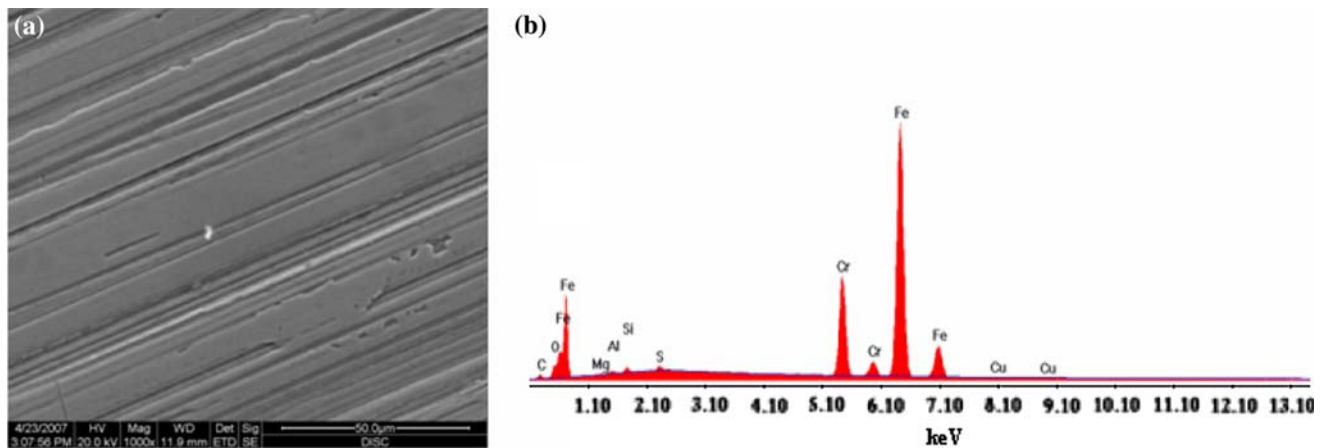


Fig. 11 SEM micrograph of worn surface of counter face disk (a); and its corresponding EDS analysis (b)

of the counter face disk using SEM is shown in Fig. 11. This figure shows the sliding direction on the SEI image, while EDS analysis indicates the formation of MML on the disk surface [19–20].

Conclusions

The following conclusions can be drawn from the present investigation:

1. The wear rate decreases with increase in hardness of Al-based alloys and composites. Wear resistance of Al-4 wt% Mg alloy improves significantly after addition of copper and/or silicon carbide particles.
2. The wear rate of the matrix alloy and the composites almost increased linearly with increasing the sliding distance. But wear rates of the P/M Al–Mg–Cu–SiC components were much smaller than that of Al–Mg–Cu components.
3. In the case of additions of copper to Al-4 wt% Mg alloy (up to 5%) both hardness and wear resistance were increased considerably because of solution hardening; on the other hand, insignificant increase in the coefficient of friction values was observed. The significant wear resistance was observed by introducing SiC particles to Al–Mg–Cu specimens. The presence of SiCP in tribofilm between two contacted surfaces results in three-body abrasion system, which increased the coefficient of friction.
4. The formations of MML as a result of material transfer from counter face disk to the samples and vice versa were observed in testing both Al–Mg–Cu and Al–Mg–Cu/SiC components.

Acknowledgements The authors gratefully acknowledge the assistance of the Committee of Scientific Research/Jordan University of Science and Technology for its support of this research (grant no. 29/2007). The authors would like also to gratefully acknowledge the use of Machine shop and the laboratory facilities at Jordan University of Science and Technology, Irbid, Jordan.

Appendix

Material properties and wear results of Al-4 wt.%Mg-Cu alloys and their based composites

Sample No.	Cu (wt.%)	SiC (vol.%)	Density (kg/m ³)	HV _{100g}	Avg. coefficient of friction	Cumulative mass loss (60 minutes)
1	0	0	2147.5	32.8	0.148	3.6
2	0	5	2070	36.0	0.197	2.9
3	0	10	2045	46.0	0.270	2.3
4	1	0	2216	42.7	0.153	2.4
5	1	5	2152.8	50.7	0.193	1.9
6	1	10	2122.4	63.8	0.266	1.7
7	2	0	2233.6	56.2	0.153	1.9
8	2	5	2213.6	60.7	0.220	1.4
9	2	10	2206.4	66.4	0.256	1.2
10	3	0	2184	59.4	0.162	1.7
11	3	5	2192.2	66.4	0.240	1.5
12	3	10	2233	70.2	0.274	1.2
13	4	0	2374	63.4	0.162	1.2
14	4	5	2222	70.2	0.210	1.1
15	4	10	2255	86.6	0.258	1.0
16	5	0	2266.7	69.6	0.177	1.2
17	5	5	2329.3	80.3	0.236	1.1
18	5	10	2306.5	88.2	0.274	1.1

References

1. Abouelmagd G (2004) *J Mater Process Technol* 155–156:395. doi:[10.1016/j.jmatprotec.2004.04.223](https://doi.org/10.1016/j.jmatprotec.2004.04.223)
2. Ahlatci H, Kocer T, Candan E, Cimenoglu H (2006) *Tribol Int* 39:13
3. Candan S, Bilgic E (2004) *Mater Lett* 58:2787. doi:[10.1016/j.matlet.2004.04.009](https://doi.org/10.1016/j.matlet.2004.04.009)
4. Torralba JM, da Costa CE, Velasco F (2003) *J Mater Process Technol* 133:203. doi:[10.1016/S0924-0136\(02\)00234-0](https://doi.org/10.1016/S0924-0136(02)00234-0)
5. Eksi A, Saritas S (2002) *Turk J Eng Environ Sci* 26:377
6. Sawla S, Das S (2004) *Wear* 257:555. doi:[10.1016/j.wear.2004.02.001](https://doi.org/10.1016/j.wear.2004.02.001)
7. Das S, Das S, Das K (2007) *Compos Sci Technol* 67:746. doi:[10.1016/j.compscitech.2006.05.001](https://doi.org/10.1016/j.compscitech.2006.05.001)
8. Zhang S, Wang F (2007) *J Mater Process Technol* 182:122. doi:[10.1016/j.jmatprotec.2006.07.018](https://doi.org/10.1016/j.jmatprotec.2006.07.018)
9. Ramachandra M, Radhakrishna K (2006) *Mater Sci-Poland* 24:334
10. Kim HS (1998) *Mater Sci Eng A* 251:100. doi:[10.1016/S0921-5093\(98\)00635-2](https://doi.org/10.1016/S0921-5093(98)00635-2)
11. Yamagushi K, Takakura N, Imatani S (1997) *J Mater Process Technol* 63:346
12. Mondal DP, Das S (2006) *Tribol Int* 39:470. doi:[10.1016/j.triboint.2005.03.003](https://doi.org/10.1016/j.triboint.2005.03.003)
13. Savaskan T, Hekimoglu AP, Gencaga P (2004) *Tribol Int* 37:45. doi:[10.1016/S0301-679X\(03\)00113-0](https://doi.org/10.1016/S0301-679X(03)00113-0)
14. Kok M (2006) *Composites A* 37:457
15. Kok M, Ozdin K (2007) *J Mater Process Technol* 183:301. doi:[10.1016/j.jmatprotec.2006.10.021](https://doi.org/10.1016/j.jmatprotec.2006.10.021)
16. Muratoglu M, Aksoy M (2000) *Mater Sci Eng A* 282:91. doi:[10.1016/S0921-5093\(99\)00767-4](https://doi.org/10.1016/S0921-5093(99)00767-4)
17. Natarajan N, Vijayarangan S, Rajendran I (2006) *Wear* 261:812. doi:[10.1016/j.wear.2006.01.011](https://doi.org/10.1016/j.wear.2006.01.011)
18. Rodriguez J, Poza P, Garrido MA, Rico A (2007) *Wear* 262:292. doi:[10.1016/j.wear.2006.05.006](https://doi.org/10.1016/j.wear.2006.05.006)
19. Ghazali MJ, Rainforth WM, Jones H (2005) *Wear* 250:490. doi:[10.1016/j.wear.2005.02.089](https://doi.org/10.1016/j.wear.2005.02.089)
20. Ghazali MJ, Rainforth WM, Jones H (2007) *Tribol Int* 40:160